

Utilization of Expired Zidovudine for Corrosion Protection

*¹S. Bulama. ¹A. M. Kolo. ¹I. Y. Chindo, ¹A. A. Mahmoud and ²S.B. Ali

¹Department of Chemistry, Abubakar Tafawa Balewa University, Bauchi, Bauchi State, Nigeria.

²Department of Chemistry Nigerian Army University, Bui, Borno State Nigeria.

*Corresponding Author: sbulama3.sb@gmail.com

Accepted: March 3, 2026. Published Online: March 12, 2026

ABSTRACT

The reutilization of pharmaceutical waste as environmentally benign corrosion inhibitors represents a promising strategy for sustainable materials protection. In this study, expired Zidovudine (AZT) was evaluated as a green corrosion inhibitor for API 5L X65 mild steel in 1.0 mol dm⁻³ HCl solution over the temperature range 303–333 K. The inhibition performance was investigated using weight loss measurements. Results revealed a maximum inhibition efficiency of 68.10% at the optimum inhibitor concentration. The inhibition efficiency decreased slightly with increasing temperature, suggesting predominant physical adsorption of inhibitor molecules onto the mild steel surface. Adsorption of AZT on the steel surface obeyed the Temkin adsorption isotherm, and calculated thermodynamic parameters confirmed a spontaneous adsorption process. Surface analyses further supported the formation of a protective adsorbed film, attributed to the presence of heteroatoms (N and O) and π -electron systems within the AZT molecular structure, facilitating interaction with the metal surface. The findings demonstrate that expired AZT exhibits appreciable corrosion inhibition efficiency and can serve as a cost-effective and sustainable alternative for corrosion control, while offering a value-added application for pharmaceutical waste management.

Key words: API 5L X65 steel, HCl, Temkin isotherm, Weight loss, Zidovudine.

INTRODUCTION

Corrosion is a pervasive and costly degradation process that affects metallic materials across virtually every industrial sector, from energy and transportation to infrastructure and manufacturing. At its core, corrosion is a spontaneous electrochemical or chemical interaction between a material—most commonly a metal—and its surrounding environment, leading to the gradual transformation of the material into more thermodynamically stable compounds such as oxides, hydroxides, or sulfides. This process not only compromises structural integrity and

functionality but also imposes significant economic, environmental, and safety burdens worldwide [1–3].

The global impact of corrosion is substantial. A comprehensive international study conducted by NACE International estimated the annual global cost of corrosion to be approximately 3–4% of the world's gross domestic product [1]. Beyond direct repair and replacement costs, corrosion contributes to unplanned shutdowns, loss of efficiency, environmental contamination, and catastrophic failures in critical infrastructure systems, including pipelines, offshore platforms, reinforced concrete structures, and transportation networks [2,3].

Corrosion phenomena are diverse and strongly dependent on material composition, environmental conditions, and mechanical stresses. Common forms include uniform corrosion, galvanic corrosion, pitting corrosion, crevice corrosion, intergranular corrosion, and stress corrosion cracking. These degradation modes are governed by electrochemical reactions occurring at the metal–environment interface and are influenced by variables such as temperature, humidity, pH, dissolved oxygen, salinity, and the presence of aggressive ions such as chlorides or sulfides [2, 4].

The complexity of these interacting factors necessitates a multidisciplinary approach integrating electrochemistry, materials science, surface engineering, and structural mechanics. Over the past decades, significant advances in corrosion science and engineering have enabled the development of effective mitigation strategies. These include the application of protective coatings, cathodic and anodic protection systems, corrosion inhibitors, improved alloy design, and advanced surface modification techniques [3–5].

In spite of the promising potential of pharmaceutical waste materials, there remains a significant research gap in understanding the application of expired drugs like AZT in corrosion inhibition. While several studies have investigated the use of organic compounds, synthetic chemicals and classes of drugs for this purpose, no comprehensive research has been conducted on the use of expired AZT in corrosion protection.

This paper aims to contribute to the ongoing effort to identify environmentally sustainable corrosion protection solutions by investigating the corrosion inhibition performance of expired AZT for mild steel. Specifically, it seeks to evaluate the effectiveness of expired AZT as a corrosion inhibitor, comparing its performance to traditional corrosion inhibitors. In doing so, the paper will explore the mechanisms through which AZT interacts with mild steel, its long-term

stability, and its potential as a cost-effective, environmentally sustainable alternative to conventional inhibitors.

MATERIALS AND METHODS

Materials and Reagents

API 5L X65 steel with chemical composition (weight %) C; 0.16, Mn; 1.65, P; 0.02, S; 0.45, Si; 0.50, Ni; 0.50, Cr; 0.05, Mo; 0.50, Al; 0.06, Cu; 0.50, V; 0.09, Nb; 0.05, B; 0.005, Ti; 0.06, N; 0.12, and Fe, 97.04 was obtained from Kaduna refinery and petrochemical limited (KRPC), Kaduna State Nigeria. Manufactured by Vallourec Brasil and supplied to Daewoo E&C Nigeria Ltd., for the quick fix repair of the refinery and petrochemical company in Kaduna. Analytical grade hydrochloric acid (HCl). Zidovudine (50 mg/ 5 mL), Aurobindo India. Expired 03/2021 was used as received from Abubakar Tafawa Balewa University Teaching Hospital. ARD clinic, and various concentrations (50, 100, 150, 200, and 250 mg L⁻¹) were prepared in the acidic medium.

All experiments were conducted at temperatures of 303, 313, 323, and 333 ± 1 K using a thermostatically controlled water bath. Fresh solutions were prepared prior to each experiment.

Preparation of Metal Specimens

A standard procedure ASTM [6], was adopted for the coupon preparation. The steel was mechanically cut into a dimension of 3 x 1 x 0.1 cm coupons.

Prior to the measurement, the specimens were mechanically polished with successive grades of silicon carbide abrasive papers (400–1200 grit), rinsed thoroughly with distilled water, degreased with ethanol, washed with acetone, dried, and stored in a desiccator until use.

Preparation of the Inhibited Solution

AZT was available as a syrup with a strength of 5 mL equivalent to 50 mg. A total of 5, 10, 15, 20, and 25 mL of the drug was measured and transferred into a different 1 L volumetric flasks containing approximately 500 mL of 1.0 mol dm⁻³ HCl solution each. The mixture was shaken vigorously, and then 1.0 mol dm⁻³ HCl solution was added to the mark.

Weight Loss Measurements

Gravimetric measurements were carried out by immersing pre-weighed mild steel coupons in 200 mL of 1.0 mol dm⁻³ HCl solution in the absence and presence of different concentrations of AZT (50–250 mg L⁻¹). The immersion period was fixed at 3 h for all experiments.

At the end of the exposure time, the specimens were retrieved, rinsed with distilled water, and the corrosion products were removed by immersion in 20% NaOH solution containing 100 g L⁻¹ zinc dust for 2–5 min [7]. The cleaned coupons were washed under running tap water using a hard bristled brush, rinsed with distilled water, degreased with ethanol, washed with acetone, dried, and accurately reweighed. All measurements were performed in triplicate, and the average weight loss values were reported.

To determine the weight loss due to corrosion, the initial and final weights of the mild steel specimen are measured. The weight loss (w) is calculated by subtracting the final weight from the initial weight of the specimen. The equation for weight loss is as follows:

$$W_i - W_f = w \quad (1)$$

where w is total weight loss, W_i and W_f are the initial weight before immersion and after respectively.

To quantify the corrosion rate of mild steel in the absence and presence of the corrosion inhibitor, we use the formula presented by [8], which relates the corrosion rate to the total weight loss and period of immersion:

$$\text{Corrosion rate (mmpy)} = \frac{87.6w}{DAT} \quad (2)$$

where w = Total weight loss (mg), D = density of specimen (g/cm³), A = Area of specimen (square meter) and T = period of immersion (hour) and 87.6 is a conversion factor.

The density of the API 5L x 65 is 7.85 g/cm³.

To determine the effectiveness of the corrosion inhibitor, the surface coverage (θ) is calculated using the ratio of the weight loss of mild steel in the presence and absence of the inhibitor and subtract from one. The surface coverage represents the fraction of the metal surface that is covered by the inhibitor molecules, which prevents the electrochemical reactions responsible for corrosion. The formula for calculating surface coverage is given by:

$$\theta = \left(1 - \frac{w_1}{w_2}\right) \quad (3)$$

where; w_1 and w_2 are the weight losses (g) for metal in the presence and absence of inhibitor respectively [8].

The inhibition efficiency (%IE) quantifies the extent to which the corrosion rate is reduced by the presence of an inhibitor. It is calculated by multiplying the value of surface coverage by 100 [8]. A higher value of %IE indicates a more effective inhibitor. The formula for inhibition efficiency is given by:

$$\%IE = \left(1 - \frac{w_1}{w_2}\right) \times 100 \quad (4)$$

RESULTS AND DISCUSSION

Weight Loss Studies

The corrosion rate (CR) and inhibition efficiency (IE%) values obtained from gravimetric measurements for mild steel in 1.0 mol dm⁻³ HCl in the absence and presence of different concentrations of AZT at various temperatures are presented in Table 1.

Table 1: The Corrosion parameters of API 5L X 65 mild steel from weight loss measurement.

Inh. (mg/L)	Surface Coverage				Corrosion Rate (mm/yr)				Inhibition efficiency			
	303K	313K	323K	333K	303 K	313 K	323 K	333 K	303 K	313K	323K	333K
Blank	-	-	-	-	0.0089	0.0137	0.0226	0.0606	-	-	-	-
50	0.136	0.128	0.098	0.072	0.0077	0.0120	0.0204	0.0562	13.60	12.80	9.80	7.20
100	0.409	0.324	0.185	0.147	0.0053	0.0093	0.0184	0.0517	40.90	32.40	18.50	14.70
150	0.500	0.422	0.281	0.227	0.0044	0.0080	0.0163	0.0469	50.00	42.20	28.10	22.70
200	0.590	0.482	0.340	0.280	0.0036	0.0071	0.0149	0.0436	59.00	48.20	34.00	28.70
250	0.681	0.647	0.429	0.327	0.0028	0.0048	0.0129	0.0408	68.10	64.70	42.90	32.70

The results show that the corrosion rate decreased significantly with increasing inhibitor concentration, indicating effective adsorption of AZT molecules on the mild steel surface. The increase in inhibition efficiency with concentration is commonly attributed to progressive surface coverage of the metal by adsorbed inhibitor molecules, which block active corrosion sites and reduce metal dissolution [9]. The inhibition efficiency increased progressively with concentration, reaching a maximum value of 68.10% at 250 mg L⁻¹ at 303 K.

However, increasing the temperature from 303 to 333 K led to an increase in corrosion rate and a corresponding decrease in inhibition efficiency. Such behavior is frequently reported for inhibitors predominantly adsorbed through electrostatic interactions, where elevated temperature promotes desorption of physically adsorbed molecules from the metal surface [10, 11]. The reduction in efficiency at higher temperatures therefore suggests that the adsorption process involves a significant physical adsorption component.

The decrease in corrosion rate in the presence of AZT confirms its protective action through the formation of an adsorbed barrier film that isolates the metal surface from the aggressive acidic medium. The formation of such a protective layer reduces both anodic metal dissolution and cathodic hydrogen evolution reactions, thereby lowering the overall corrosion rate [11, 12].

Thermodynamic and Adsorption behavior

The adsorption of AZT on the mild steel surface was analyzed using thermodynamic parameters, which provide insight into the nature of the adsorption process and the stability of the inhibitor-metal interface. The surface coverage (θ) obtained from weight loss measurements was used to calculate the adsorption equilibrium constant (K_{ads}) according to the Temkin adsorption isotherm [12]:

$$\theta = -\frac{2.303}{2\alpha} \log K_{ads} - \frac{2.303}{2\alpha} \log C \quad (5)$$

Where C is the inhibitor concentration and θ is the surface coverage. Linear plot of θ versus $\log C$ produce a straight line with slope and intercept equal to $-\frac{2.303}{2\alpha}$ and $-\frac{2.303}{2\alpha} \log K_{ads}$ respectively, confirmed that the adsorption of AZT obeys the Temkin adsorption isotherm (Fig. 1) suggesting multilayer adsorption.

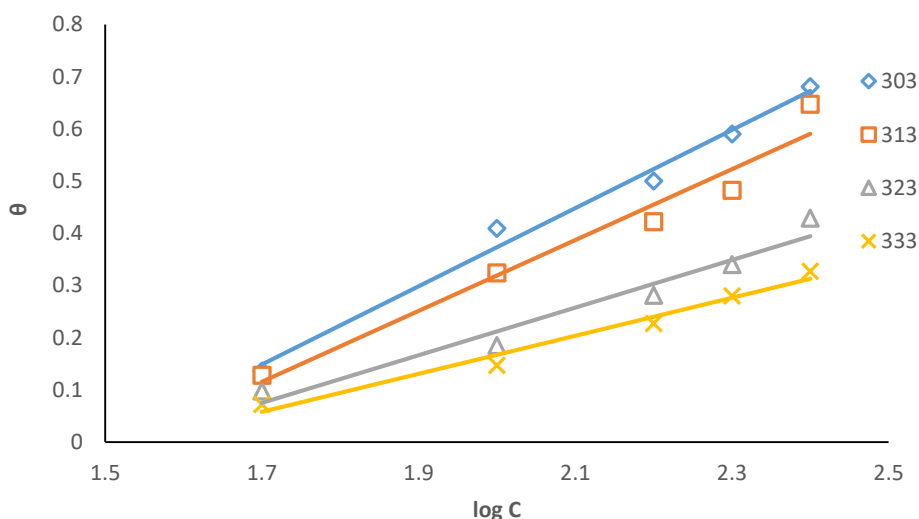


Figure 1: Temkin adsorption Isotherm of AZT

Adsorption Free Energy

To predict the spontaneity of the corrosion process, the Gibbs free energy change (ΔG) is calculated. A negative value of ΔG indicates that the corrosion reaction is spontaneous, while a positive value suggests that the reaction is not spontaneous [13].

$$\Delta G_{\text{ads}}^{\circ} = -2.303RT \log(55.5K_{\text{ads}}) \quad (6)$$

where R is the gas constant ($8.314 \text{ J}\cdot\text{mol}^{-1}\cdot\text{K}^{-1}$), T is the absolute temperature (K), and 55.5 is the molar concentration of water in solution.

Activation Energy (E_a)

The activation energy (E_a) is a crucial parameter in understanding the temperature dependence of the corrosion rate. It quantifies the energy barrier that must be overcome for the corrosion reaction to occur. The Arrhenius equation is commonly used to describe the relationship between the corrosion rate and temperature. The activation energy can be determined from the slope of an Arrhenius plot of the corrosion rate against the reciprocal temperature. The equation for the corrosion rate as a function of temperature is given by:

$$k = A, e^{-\frac{E_a}{RT}} \quad (7)$$

or

$$\log CR = -\frac{E_a}{2.303RT} + \log A \quad (8)$$

where CR is corrosion rate, R the molar gas constant (8.314 J/mol/K), T is the absolute temperature and A is the Arrhenius constant respectively [14].

To calculate the activation energy, a plot of natural logarithm of the corrosion rate ($\log CR$) versus $1/T$ the slope of the resulting lines (Fig. 2) gives the value of $-\frac{E_a}{2.303RT}$. From this, the activation energy values were evaluated and reported in Table 2.

Activation Parameters

The Van't Hoff equation is used to relate the temperature dependence of the rate constant (or corrosion rate) [15]. By examining the temperature dependence, the activation parameters such as the enthalpy and entropy of activation can be extracted. The equation is given by:

$$\log \frac{CR}{T} = \left[\log \left(\frac{R}{Nh} \right) + \frac{\Delta S^*}{2.303R} \right] - \frac{\Delta H^*}{2.303RT} \quad (9)$$

where h is the plank's constant and N is the Avogadro's number, respectively.

A plot of $\log \frac{CR}{T}$ versus $\frac{1}{T}$ gave a straight line with a slope of $\frac{-\Delta H^*}{2.303R}$ and intercept of $[\log \left(\frac{R}{Nh} \right) + \frac{\Delta S^*}{2.303R}]$, from which the activation thermodynamics parameters (ΔH^*) and (ΔS^*) were evaluated (Fig. 3).

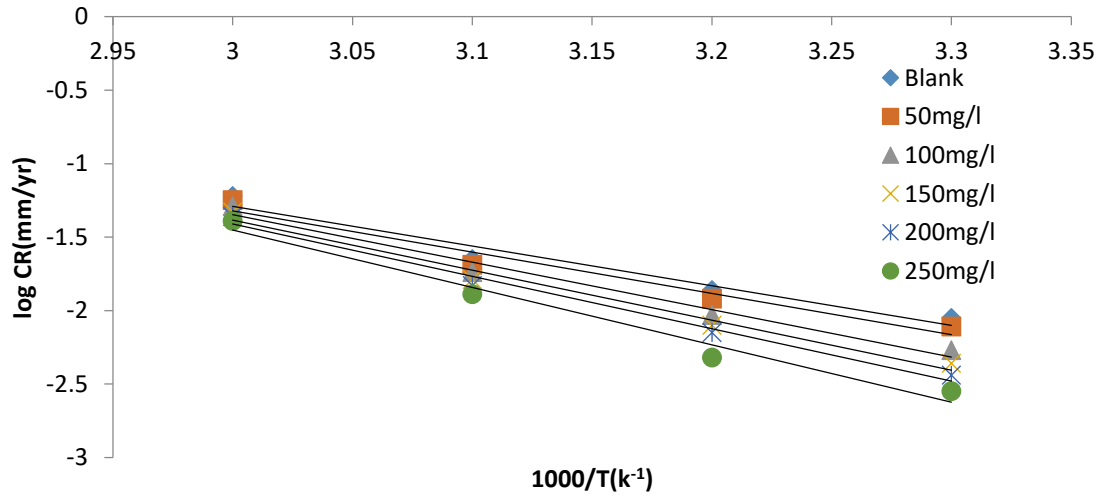


Figure. 2: Arrhenius plot for AZT

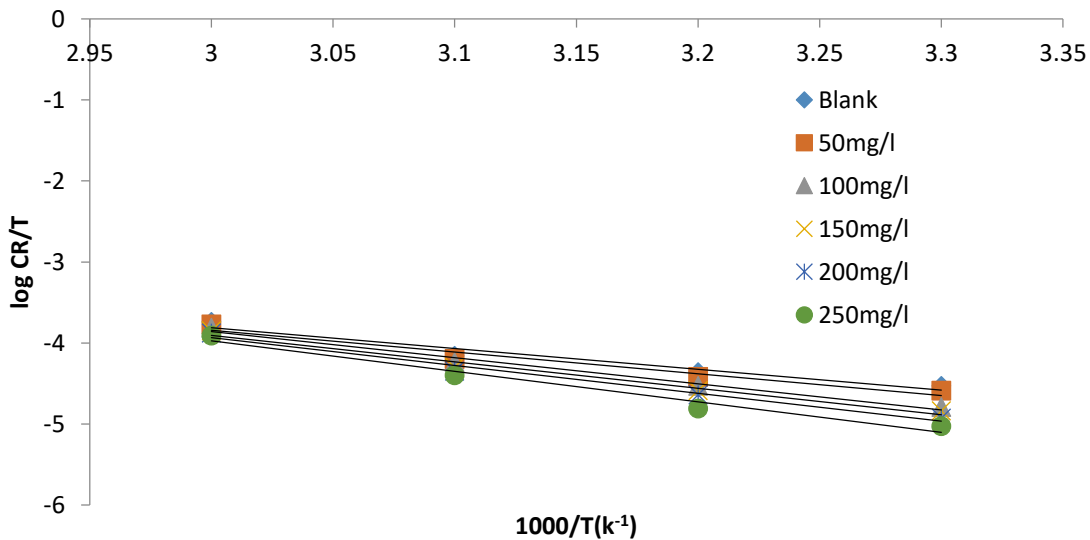


Figure. 3: Transition state plot for AZT.

Tables 2 and 3, summarize the thermodynamic and Temkin absorption parameters.

Table. 2: Kinetic and thermodynamic parameters for corrosion inhibition of API 5L X65 mild steel in absence and present of an inhibitor.

Inhibitor Conc.(mg/L)	E_a (kJ/mol)	$-\Delta H^*$ (kJ/mol)	$-\Delta S^*$ (kJ/mol)
Blank	51.71	49.23	272.27
50	53.81	51.32	277.87
100	61.85	61.85	309.08
150	65.11	62.43	310.12
200	68.17	65.88	319.92
250	74.88	72.20	338.15

Table. 3: Isotherm parameters for the Adsorption of inhibitor on to the surface of API 5L X65 steel in 1.0 M HCl at various Temperatures.

Adsorption Isotherm	Inhibitor	Temp (K)	Slope	Intercept	K_{ads}	α	ΔG_{ads} (kJmol ⁻¹)	R ²
Temkin	AZT	303	0.7490	-1.1246	31.92	-1.54	-18.85	0.9880
		313	0.6787	-1.0382	34.10	-1.70	-19.64	0.9588
		323	0.4560	-0.7001	34.57	-2.53	-20.31	0.9550
		333	0.3644	-0.5620	34.86	-3.16	-20.97	0.9764

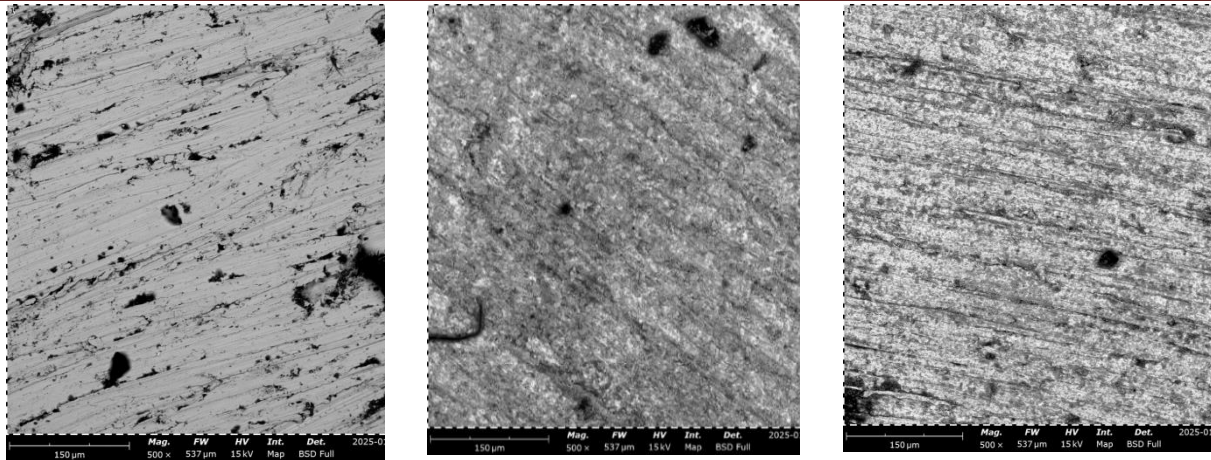
A negative ΔH^*_{ads} value confirms that the adsorption process is exothermic and ΔS^*_{ads} indicates an increase in disorder at the metal-solution interface due to replacement of water molecules by inhibitor molecules [16].

The calculated ΔG^o_{ads} values fall in the range of -18 to -21 kJ/mol, indicating that Zidovudine adsorption is spontaneous. Since the ΔG^o_{ads} value falls below -40 kJ/mol, it suggests that the adsorption involves physisorption [17, 18].

Overall, the thermodynamic analysis confirms that Zidovudine adsorbs spontaneously on the mild steel surface through a physical interaction, forming a protective multilayer that inhibits corrosion in acidic media.

Surface Analysis: SEM-EDX

The effect of AZT on the surface morphology of mild steel in 1.0 mol dm⁻³ HCl was investigated using Scanning Electron Microscopy (SEM). Fig. 4 shows the SEM images of mild steel surfaces after 24 h immersion in the absence and presence of 250 mg/L AZT.



SEM image of untreated coupon surface

SEM image of Coupon treated with acid (blank)

SEM image in the presence of AZT

Figure 4: SEM image of mild steel surface in absence and presence of AZT

In the blank solution, the steel surface was severely corroded, exhibiting deep pits and rough morphology due to aggressiveness of the acid environment. This confirms the high corrosion rate observed from weight loss. In the presence of AZT, the surface appeared significantly smoother, with fewer pits and a more uniform layer, indicating the formation of a protective film on the steel surface and block the active corrosion site [19].

EDX Analysis

The elemental composition of the steel surface was analyzed using Energy Dispersive X-ray Spectroscopy (EDX) to detect changes after inhibitor adsorption. The EDX spectrum of the blank surface (Fig. 5) showed a high percentage of Fe and Cl, confirming the penetration of chloride ions and extensive corrosion. After immersion in the presence of the inhibitor, the EDX spectrum (Fig. 6) revealed, reduced intensity of Cl, indicating less chloride attack. Appearance of N, and O peaks, confirming the adsorption of AZT molecules on the metal surface [20-22].

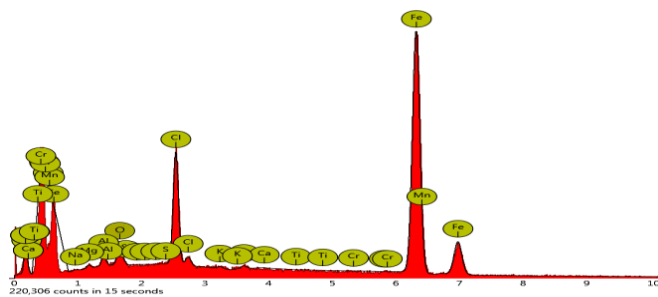


Figure. 5: EDX spectrum of treated API 5L X65 steel in the presence acid (uninhibited).

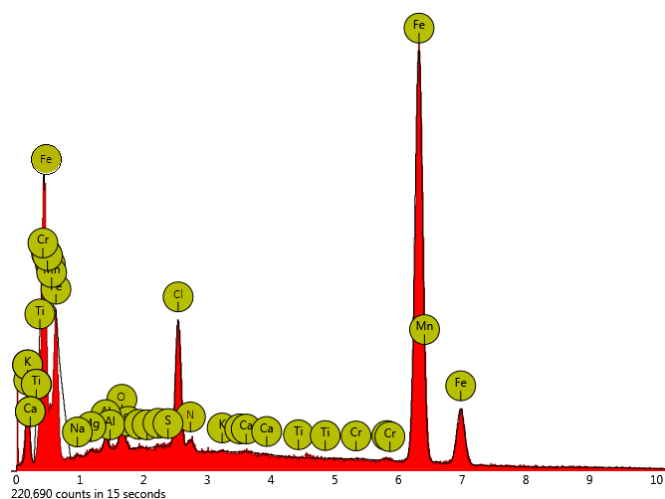


Figure. 6: EDX spectrum of treated API 5L X65 steel in the presence of AZT drug.

The SEM-EDX results, therefore, provide strong evidence that AZT forms a protective adsorbed layer, reducing metal dissolution and improving corrosion resistance in acidic medium.

CONCLUSION

The results obtained from the weight loss measurements and SEM–EDX analyses demonstrate the effective corrosion inhibition performance of AZT on steel in 1.0 mol dm^{-3} HCl acid solution.

Weight loss studies revealed that the corrosion rate of steel decreased significantly with the addition of AZT, while inhibition efficiency increased with inhibitor concentration. This behavior indicates that AZT molecules adsorb onto the steel surface, forming a protective barrier that limits direct contact between the metal and the aggressive chlorine ions.

Surface morphology examination by SEM supported these findings. The steel surface exposed to the blank solution showed severe damage characterized by deep pits and rough morphology, confirming intense corrosive attack. In contrast, the surface immersed in the AZT-containing solution appeared much smoother and more uniform, with fewer defects, indicating the formation of a protective adsorbed film.

Furthermore, EDX analysis confirmed the adsorption mechanism. The blank sample exhibited strong Fe and Cl signals, indicating significant chloride penetration and corrosion. After treatment with AZT, the intensity of Cl decreased markedly, while additional N and O signals appeared, confirming the presence of inhibitor molecules on the steel surface.

Overall, the combined weight loss and SEM–EDX results confirm that AZT acts as an efficient corrosion inhibitor by adsorbing onto the steel surface and blocking active corrosion sites, thereby reducing metal dissolution and acid attack.

REFERENCES

- [1] Koch, G. H., Varney, J., Thompson, N., Moghissi, O., Gould, M. & Payer, J. (2016). *International Measures of Prevention, Application, and Economics of Corrosion Technologies Study (IMPACT)*. NACE International.
- [2] Revie, R. W & Uhlig, H. H. (2008). *Uhlig's Corrosion Handbook* (3rd ed.). John Wiley & Sons.
- [3] Jones, D. A. (1996). *Principles and Prevention of Corrosion* (2nd ed.). Prentice Hall.
- [4] Fontana, M. G. (2005). *Corrosion Engineering* (3rd ed.). McGraw-Hill.
- [5] Schweitzer, P. A. (2010). *Fundamentals of Corrosion: Mechanisms, Causes, and Preventative Methods*. CRC Press.
- [6] ASTM (American Society for Testing and Materials) International, G-1. (1999). *Standard practice for preparing, cleaning and evaluation corrosion test specimens*. Annual Book of ASTM standard, 2(1), 15-21.
- [7] ASTM (American Society for Testing and Materials) International, G1-90 (1999) e1. *Standard practice for preparing, cleaning and evaluation corrosion test specimens*. Annual Book of ASTM standard, 1-4.
- [8] Onen., A. I., Bulama, S., Kolo, A. M., Ebenso, E. E. & Apagu, D. A. (2019). Gravimetric and Electrochemical Studies of *Balanitea egyptiaca* DEL. Ethanolic Leaves Extract as Corrosion Inhibitor for Duplex Stainless Steel (DSS) in 1.0M HCl Solution. *FUW Trends Journal in Science and Technology*. 4 (3), 773 – 777.
- [9] Quraishi, M.A. & Sardar R. (2002). Corrosion inhibition of mild steel in acid solutions by some aromatic oxadiazoles, *Corrosion Science*, 44, 197–207.
- [10] Raja, P.B. & Sethuraman M.G. (2008). Natural products as corrosion inhibitor for metals in corrosive media – A review, *Materials Letters*, 62, 113–116.
- [11] Obot, I.B. & Obi-Egbedi N.O. (2010). Adsorption properties and inhibition of mild steel corrosion in sulphuric acid solution by ketoconazole, *Corrosion Science*, 52, 198–204.
- [12] El-Etre, A.Y. (2007). Inhibition of acid corrosion of carbon steel using aqueous extract of olive leaves, *Journal of Colloid and Interface Science*, 314, 578–583.

- [13] Sharma, S. K., Mudhoo, A., Jain, G & Sharma, J. (2010). Corrosion Inhibition and Adsorption properties of Azadirachta indica mature leaves extract as green inhibitor for Mild steel in Nitric Acid. *Green Chemistry Letters and Reviews* **3**(1): 7-15.
- [14] Nsude, O. P & Orié, K. J. (2022). Thermodynamic and Adsorption Analysis of Corrosion Inhibition of Mild Steel in 0.5M HCl Medium via Ethanol Extracts of *Phyllanthus mellerianus*. *American Journal of Applied Chemistry*. 10(3): 67-75.
- [15] Karthik. G. and Sundaravadivelu. M. (2015) Studies on the inhibition of mild steel corrosion in hydrochloric acid solution by atenolol drug. *Egyptian Journal of Petroleum* **25**, 183–191.
- [16] El-Awady, A.A., Abd-El-Nabey, A.B and Aziz S.G. (1999). Kinetics-Thermodynamic and Absorption isotherms analysis for the Inhibition of Acid corrosion of Steel by cyclic and open chain Amines. *Journal of Electrochemical Society* **139**(8) 2149-2154
- [17] Onen, A. I., Nwufu, B. T & Ebenso, E. E. (2011). The effect of *Cassia siamea* Lam. Root Extract on the Corrosion and Kinetics of Corrosion process of Copper in Alkaline solution. *E- Journal of Chemistry*, 8(4), 1708-1713.
- [18] Sudheer and Quraishi, M. A. (2011). Effect of pharmaceutically active compound Omeprazole, on the corrosion of mild steel in hydrochloric acid solution. *Journal of Chemical and Pharmaceutical Research*. **3**(5):82-92
- [19] Khamis, M. Abd El-Rehim S. & El-Shamy, A. M. (2016) .Mechanistic study of mixed-type inhibitors on steel corrosion, *Journal of Applied Electrochemistry*, 46, 1051–1062.
- [20] Kolo, A. M., Kutama, I. U., Sani, U. M. & Usman, U. (2016). Electrochemical, SEM and FTIR study of the corrosion inhibition of *Januvia* for Zinc in Hydrochloric acid medium. *Journal of Apply Chemical Science International*, 6(4), 210-216.
- [21] Rosliza. R. & Izman, S. (2011) SEM-EDX Characterization of Natural Products on Corrosion Inhibition of Al-Mg-Si alloy. *Journal of Physicochemical Problems of Materials Protection* **47**: 395-401.
- [22] Schmitt, G. (2008). Adsorption of heterocyclic organic compounds on steel surfaces in acidic media, *Materials Chemistry and Physics*, 110, 1–10.